

## Momentum Distribution Dependence of Induced Electron-Cyclotron Emission

L. F. ZIEBELL and D. DILLENBURG

*Instituto de Física, Universidade Federal do Rio Grande do Sul, 90000, Porto Alegre, RS, Brasil*

Recebido em 13 de fevereiro de 1984

**Abstract** The dependence of the electron-cyclotron wave amplification in an inhomogeneous plasma slab on the electron momentum distribution is investigated. Two types of distributions are considered, both featuring a loss cone and a Maxwellian component. It is shown that the perpendicular emission at the fundamental frequency is in general greatly reduced by the presence of a Maxwellian component and situations occur in which a layer in the slab very effectively absorbs all the radiation amplified elsewhere. The transition from the pure loss cone to the pure Maxwellian case is accompanied by a peculiar behavior of the dielectric tensor components, which may invalidate the geometrical optics approximation in the calculation of the emission and the commonly held belief that the real part of the refractive index is insensitive to the shape of the momentum distribution function.

### 1. INTRODUCTION

In this paper we return to the problem of induced electron-cyclotron emission from inhomogeneous anisotropic plasmas with electron population inversion. In previous work<sup>1</sup> we have shown that the resulting amplified emission near the fundamental frequency is sensitively dependent on the ratio of parallel to perpendicular temperature and on inhomogeneities in the magnetic field. The electrons were represented by the distribution function, normalized to one,

$$f_{\ell}(p_{\perp}, p_{\parallel}) = A_{\ell} p_{\perp}^{2\ell} \exp\{-\mu_{\perp\ell} p_{\perp}^2/b - \mu_{\parallel\ell} p_{\parallel}^2/b\} \quad (1)$$

where  $p_{\perp}$  and  $p_{\parallel}$  denote the momentum of the electrons in the directions, respectively, perpendicular and parallel to the magnetic field,

$$A_{\ell} = \frac{\mu_{\perp\ell}^{\ell+1} \mu_{\parallel\ell}^{1/2}}{b^{\ell+3/2} \pi^{3/2} \ell!}, \quad b = 2 (mc)^2$$

$$\mu_{\perp\ell} = \frac{mc^2}{T_{\perp\ell}}, \quad \mu_{\parallel\ell} = \frac{mc^2}{T_{\parallel\ell}},$$

$m$  is the electron mass,  $c$  the velocity of light,  $T_{\perp}$  and  $T_{\parallel}$  are the

perpendicular and parallel temperatures given in units of energy;  $R$  is an integer parameter greater than or equal to zero.

In the present work we emphasize the dependence of the induced radiation on the distribution function. To some extent, the parameter  $\ell$  in Eq. (1) exemplifies this dependence. However, in more realistic situations quite different types of distributions can be envisaged, and we consider two of them here.

The first type is a partially filled up loss cone. One would expect such a distribution to occur in physical situations as a consequence of collisions and/or turbulence-generated instabilities. The second is a superposition of a low temperature Maxwellian component and a high energy loss cone component. This might describe certain equilibrium states of magnetically confined plasmas with particle velocity distributions far from thermodynamic equilibrium<sup>2,3</sup>.

To investigate the induced emission due to these two types of distributions we rely strongly on the formulation of our earlier paper<sup>1</sup>. In Sec. 2 we briefly restate the model, assumptions and expressions used there, indicating the modifications which are pertinent to the present case. In Sec. 3 we proceed to the numerical analysis, discussion of results, and conclusions.

## 2. PHYSICAL MODEL AND ANALYTIC RESULTS

We consider perpendicular propagation of electron-cyclotron waves in a plasma slab, obtain the absorption coefficient for these waves by solving the dispersion relation, and calculate their emission from the slab surface by integrating the Poynting vector along the radiation path. The magnetic field is taken parallel to the slab faces. The coordinates are chosen such that the  $z$  axis is parallel to the field and the  $x$  axis perpendicular to the slab boundaries. The plasma parameters are smoothly inhomogeneous along the  $x$  direction. Radiation of frequency  $\omega < \Omega_e$  propagates along  $x$ , so that the wave vector is  $\vec{k} = k\hat{x}$ . The radiation fields are obtained as a WKB solution of Maxwell's equations in a weakly relativistic medium which is homogeneous in the  $y$  and  $z$  directions and stationary in time. The dielectric tensor elements are calculated in the local approximation and to lowest relevant order in the Larmor radius expansions.

To calculate the current correlation tensor, the typical length scale of significant current correlations is assumed to be much smaller than the typical length scale of variation of the plasma parameters. For the real ( $N'$ ) and imaginary ( $N''$ ) parts of the index of refraction ( $N$ ), the relation  $|N''| \ll |N'|$  is assumed. The resulting expressions for the power radiated per units of slab area, solid angle and angular frequency, for the ordinary ( $I_o$ ) and the extraordinary mode ( $I_x$ ) are, respectively <sup>4</sup>,

$$I_o = \left(\frac{2\pi}{c}\right)^2 \frac{\omega^2}{c} \int_{-a}^a \frac{G_{zz}}{|1 - \chi_{zz}|^2 |N_o|} \exp\left(-\frac{2\omega}{c} \int_x^a N''(x') dx'\right) (2)$$

$$I_x = \left(\frac{2\pi}{c}\right)^2 \frac{\omega^2}{c} \int_{-a}^a dx \frac{|\epsilon_{xx} - i\epsilon_{xy}|^2}{|\epsilon_{xx}|^2 |N_x|} G_{xx} \exp\left(-\frac{2\omega}{c} \int_x^a N''(x') dx'\right) (3)$$

Propagation is from the slab surface at  $x=-a$  to the surface at  $x=+a$ , with no externally incident radiation considered. The notation is as defined in Ref.1.

The indices of refraction (squared) are given by

$$N_o^2 = \epsilon_{zz} / (1 - \chi_{zz}), \quad N_x^2 = (\epsilon_{xx}^2 + \epsilon_{xy}^2) / \epsilon_{xx} \quad (4)$$

We assume that positive  $N_o$  and  $N_x$  represent propagation in the positive direction of  $x$ , and negative  $N_o$  and  $N_x$  represent propagation in the negative direction of  $x$ .

The two electron distribution functions envisaged in the Introduction will be denoted by  $f^I$  (partially filled up loss cone) and  $f^{II}$  (high energy loss cone plus low temperature Maxwellian), and will have in common the form

$$\mathbf{f} = \rho_0 f_o + (1 - \rho_0) f_\ell \quad (5)$$

where  $\rho_0$  ( $0 \leq \rho_0 \leq 1$ ) represents the fraction of Maxwellian electrons ( $\ell=0$ );  $\mathbf{f}$ , and  $f_\ell$  are defined by Eq.(1).

The dielectric tensor elements, obtained from Ref. 5 are, for perpendicular propagation,

$$\begin{aligned} \epsilon_{\alpha\beta} = & \delta_{\alpha\beta} + X \int_{n=-\infty}^{\infty} d^3p \frac{p_{\perp}^{\pi^*} \pi_{\alpha n} \pi_{\beta n}}{\gamma + nY} \frac{\partial f}{\partial p_{\perp}} \\ & + X \delta_{\alpha z} \delta_{\beta z} \int d^3p \frac{p_{\parallel}}{\gamma} \left[ \frac{\partial}{\partial p_{\parallel}} - \frac{p_{\parallel}}{p_{\perp}} \frac{\partial}{\partial p_{\perp}} \right] f \end{aligned} \quad (6)$$

with notation and approximations described in Ref.1.

The hermitian parts of  $\epsilon_{\alpha\beta}$  are given by

$$\begin{aligned} \epsilon'_{xx} &= \rho_0 \epsilon'_{xx,0} + (1-\rho_0) \epsilon'_{xx,l} \\ \epsilon'_{xy} &= \rho_0 \epsilon'_{xy,0} + (1-\rho_0) \epsilon'_{xy,l} \\ \epsilon'_{zz} &= \rho_0 \epsilon'_{zz,0} + (1-\rho_0) \epsilon'_{zz,l} + N^2 \left[ \rho_0 \chi'_{zz,0} + (1-\rho_0) \chi'_{zz,l} \right] \\ \epsilon'_{xz} &= \epsilon'_{zx} = 0 \quad \epsilon'_{yz} = \epsilon'_{zy} = 0 \\ \epsilon'_{xy} &= -\epsilon'_{yx} \quad \epsilon'_{yy} = \epsilon'_{xx} \end{aligned} \quad (7)$$

the antihermitian parts are given by

$$\begin{aligned} \epsilon''_{xx} &= \rho_0 \epsilon''_{xx,0} + (1-\rho_0) \epsilon''_{xx,l} \\ \epsilon''_{zz} &= N^2 \left[ \rho_0 \chi''_{zz,0} + (1-\rho_0) \chi''_{zz,l} \right] \\ \epsilon''_{yy} &\approx \epsilon''_{xx} \quad \epsilon''_{xy} = -\epsilon''_{yx} = -i\epsilon''_{xx} \\ \epsilon''_{xz} &= \epsilon''_{zx} = 0 \quad \epsilon''_{yz} = -\epsilon''_{zy} = i\epsilon''_{xz} = 0 \end{aligned} \quad (8)$$

In the expressions  $\epsilon'_{\alpha\beta,0}$ ,  $\epsilon'_{\alpha\beta,l}$ ,  $\epsilon''_{\alpha\beta,0}$  and  $\epsilon''_{\alpha\beta,l}$ , the subindices 0 and R indicate that they are calculated with the distribution function given by Eq. (i), taken with  $R = 0$  and with  $R \neq 0$ , respectively. The explicit expressions (for any  $l$ ) can be straightforwardly obtained from those given in Ref.1 by the substitution of  $\mu_{\perp l}$ ,  $\mu_{\parallel l}$  for  $\mu_{\perp}$ ,  $\mu_{\parallel}$ .

The elements of the microscopic current correlation tensor for perpendicular propagation are, from ref.6

$$G_{\alpha\beta}(\vec{k}, \omega) = \frac{\omega^2}{2m\omega} \frac{1}{(2\pi)^4} \sum_{n=-\infty}^{\infty} \int d^3p \frac{p_{\perp}^2 \pi_{\alpha n}^* \pi_{\beta n}}{\gamma} f \delta(\gamma+nY) \quad (9)$$

resulting in

$$\begin{aligned} G_{xx} &= \rho_0 G_{xx,0} + (1-\rho_0) G_{xx,\ell} \\ G_{zz} &= \rho_0 G_{zz,0} + (1-\rho_0) G_{zz,\ell} \\ G_{yy} &\approx G_{xx}, \quad G_{xy} = -G_{yx} = -iG_{xx} \\ G_{xz} &= G_{zx} = 0, \quad G_{yz} = -G_{zy} = iG_{xz} = 0. \end{aligned} \quad (10)$$

The subindices 0 and  $\ell$  in  $G_{\alpha\beta}$  have the same meaning as in  $\epsilon_{\alpha\beta}$ , and the explicit expressions are similarly obtained from the ones given in Ref.1.

Next, we proceed to the numerical analysis.

### 3. NUMERICAL RESULTS AND CONCLUSION

We choose for the plasma parameters the following profiles<sup>1</sup> in the range  $-a < x < a$ :

$$\begin{aligned} n_e(x) &= n_e(0) \left[ 1 - \frac{x^2}{a^2} \right] \\ T_{\perp,\ell}(x) &= T_{\perp,\ell}(0) \left[ 1 - \frac{x^2}{a^2} \right]^2 \\ T_{\parallel,\ell}(x) &= T_{\parallel,\ell}(0) \left[ 1 - \frac{x^2}{a^2} \right]^2 \\ B_0(x) &= B_0(\pm a) = B_0 \end{aligned} \quad (11)$$

where  $n_e(0) = 7 \times 10^{12} \text{ cm}^{-3}$ ,  $B_0 = 15 \text{ kG}$ ,  $a = 10 \text{ cm}$ . For temperatures we take:

$$\begin{aligned} \text{in } f^I, \quad T_{\perp\ell}(0) &= T_{\parallel\ell}(0) = 10 \text{ keV} \\ T_{\perp 0}(0) &= T_{\parallel 0}(0) = 10 \text{ keV} \end{aligned}$$

$$\begin{aligned} \text{in } f^{II}, T_{\perp l l}(0) &= T_{\perp l l}(0) = 10 \text{ keV} \\ T_{\perp 10}(0) &= T_{\perp 10}(0) = 0.1 \text{ keV} \end{aligned}$$

The magnetic field is assumed to be homogeneous, for simplicity.

In Ref.1, we studied the dependence of the amplification on the parameter  $l$ , up to  $l = 3$ , and on frequency, near the electron cyclotron frequency. For the present study, we take  $R = 3$ , because it exhibits more conspicuously the loss cone feature, and we fix the frequency by choosing  $Y = 1.01$ , value at which the amplification is nearly maximum for  $\rho_0 = 0$ , as shown in Ref.1.

The parameters chosen, and the whole model used, may be thought of as representing the central section of some plasma confined by magnetic mirrors<sup>7</sup>. The temperature taken for the loss cone part of the distribution function is in the thermonuclear range, but still low enough to justify our assumption of keeping only terms related to the fundamental frequency in  $E_{\alpha\beta}$  and  $G_{\alpha\beta}$  (harmonic overlap not being significant).

We start by considering distributions of type  $f^I$ . In Fig. 1 we depict the dependence of  $f^I$  on  $p_{\perp}$  (in arbitrary units) for different values of the "filling up" parameter  $\rho_0$ ; as  $\rho_0$  grows from 0 to 1,  $f^I$  evolves from a  $l = 3$  loss-cone type distribution to a Maxwellian distribution. In Figs. 2 and 3 we show the dependence of  $k'$  and  $k''$  on  $x$ , for the extraordinary mode, with  $k'$  and  $k''$  the real and imaginary parts of  $k \equiv (\omega/c) n_x$ , respectively. One observes from Fig. 2 that for  $\rho_0 = 0$ , amplification occurs over almost the entire slab width, excepting the borders<sup>1</sup>. The presence of a small fraction of Maxwellian electrons gives rise to an absorptive layer in the central region of the slab, as illustrated with the case  $\rho_0 = 0.1$ . For  $\rho_0 \gtrsim 0.4$  there is absorption over the whole slab width, with a general tendency for  $k''$  to decrease when  $\rho_0$  tends to 1. In Fig. 4 we plot

$$\eta(x) = 1 - \exp \left[ -2 \int_{-a}^x k''(x') dx' \right] ;$$

it represents the fraction of power removed from ( $\eta > 0$ ) or accrued to ( $\eta < 0$ ) the field along the ray path from  $x = -a$  to  $x$ . The absorptive layer for  $\rho_0 = 0.1$ , mentioned above, becomes so effective that all

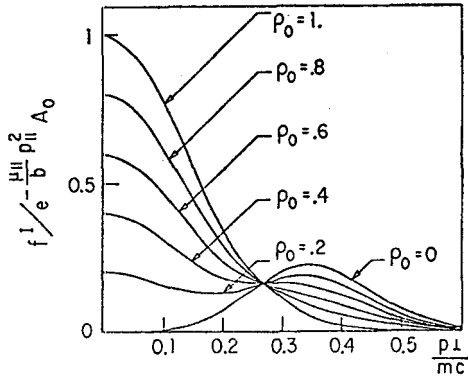


Fig.1 - Distribution function  $f^I$  versus perpendicular momenta, for different values of  $\rho_0$ .  $A_0$  and  $f^I$  are defined after Eqs. (1) and (11) respectively.

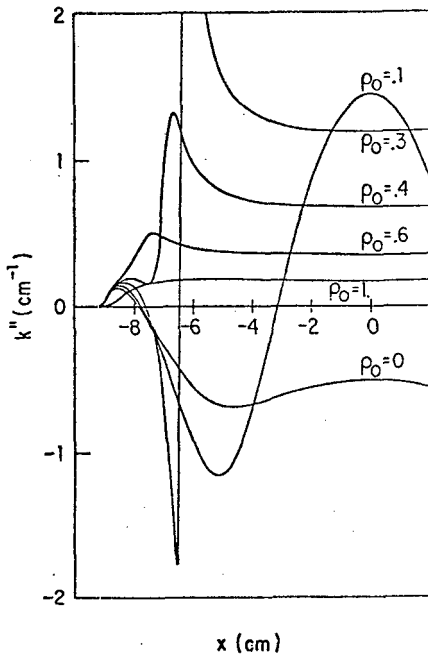


Fig.2 -  $k''$  versus  $x$  for different values of  $\rho_0$ ; distribution function  $f^I$ .

the radiation amplified elsewhere is completely reabsorbed near the central region. When  $\rho_0$  is such that there is no amplification, all the radiation is absorbed, and the length of the region of energy deposition increases with  $\rho_0$ , as seen for  $\rho_0 = 0.6$  and  $\rho_0 = 1$  in Fig. 4.

It is possible to understand qualitatively these results by considering the resonant momenta, which satisfy the condition  $\gamma - Y = 0$  and the derivative of the distribution function at resonance, for each position in the plasma slab. The arguments proceed as in Ref. 1, and are not repeated here. One new aspect to be noted in the present case is that the slope of  $f^T$  at resonance may acquire negative values in two regions of velocity space, as can be seen from Fig. 1.

For  $\rho_0$  around 0.3 the calculations show an unexpected feature which deserves some further consideration. In Fig. 3 we see that  $k'$  presents a strong variation, quite localized near the point  $x = -6$  cm in the plasma slab. From Fig. 2 we see that large values of  $k''$ , with opposite signs, occur near the same point. One would be entitled to expect a gradual vanishing of negative values of  $k''$ , as  $\rho_0$  grows from  $\rho_0 = 0$  to  $\rho_0 \approx 0.4$ , because of the disappearance of the region of positive slope in the distribution function; but instead there are sharp variations around the point where  $k''$  is zero. To see why this happens, we consider the expression

$$N''_x \approx (1/2N'_x) (\epsilon'_{xx} - i\epsilon'_{xy})^2 \epsilon''_{xx} / |\epsilon_{xx}|^2$$

which results from Eq. (4), and look for the space dependence of  $\epsilon'_{xx}$  and  $\epsilon''_{xx}$ , shown in Figs. 5 and 6. Even for a Maxwellian distribution ( $\rho_0=1$ ),  $\epsilon'_{xx}$  can change sign, as a consequence of the relativistic gyroresonance effect. Also  $\epsilon''_{xx}$  can change sign, corresponding to the fact that there are resonances at regions of positive and negative slope of the distribution function. As a consequence, both  $\epsilon'_{xx}$  and  $\epsilon''_{xx}$  can become simultaneously zero at the same point of the plasma slab. In our case, it does happen near  $x = -6.2$  cm, when  $\rho_0 \approx 0.27$ . The ratio  $\epsilon''_{xx} / |\epsilon_{xx}|^2$  can thus become very large, with both signs, which explains the fast variation of  $k''$ . This behavior could of course accidentally also occur in the case of a homogenous medium for the appropriate choice of parameters. We remark that near the region where it does happen, the behavior of  $k''$  and  $k'$  is such that it endangers the val-



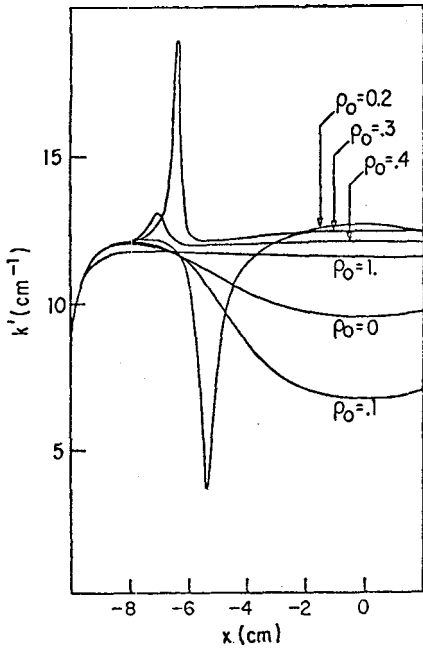


Fig.3 -  $k'$  versus  $x$  for different values of  $\rho_0$ ; distribution function  $f^I$ .

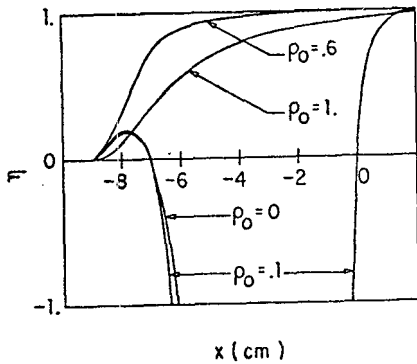


Fig.4 -  $\eta(x) = 1 - \exp[-2 \int_{-a}^x k'' dx]$  versus  $x$ , for different values of  $\rho_0$ ; distribution function  $f^I$ .

idity of the WKB solution and the expressions for the intensity of emission, presented in Ref.1. Particularly, the condition  $|k''| \ll |k'|$  may be violated.

In Table I we give the amplification of the emission at  $x = a$  for different values of  $\rho_0$ , defined as  $A_{\rho_0} = 10 \log (I_{x, \rho_0} / I_{x, 0})$ , where  $I_{x, \rho_0}$  refers to Eq. (3) for a given value  $\rho_0$ . The calculation is limited to values of  $\rho_0$  for which  $k'$  and  $k''$  satisfy the required behavior. One observes that for small values of  $\rho_0$  the emission is first increased and then greatly reduced, while as  $\rho_0$  approaches 1 it becomes rather insensitive to  $\rho_0$ , essentially because the optical depth is then much smaller than the slab width.

Table I -  $A_{\rho_0}$  for several values of  $\rho_0$ ; distribution function  $f^I$ .

| $\rho_0$ | $A_{\rho_0}$ |
|----------|--------------|
| 0        | 0.0          |
| 0.05     | 4.3          |
| 0.1      | -28.4        |
| 0.6      | -68.9        |
| 0.8      | -69.9        |
| 1.0      | -69.4        |

Next, we analyze the results for a distribution of type  $f^{II}$ . In this case we have a very cold Maxwellian admixed to a  $\lambda=3$  loss-cone distribution, which is difficult to draw to scale. As fig. 7 shows, the medium does not become absorptive in this situation, for the frequency considered, except near the surface. The reason is that the second region of negative slope of the distribution function occurs only for very small values of  $p_{\perp}$ , for which there is no significant resonance. Again a large variation of  $k''$  is evident, and occurs at the point  $x \approx -7.8 \text{ cm}$  for  $\rho_0 \approx 0.7$ , while  $k'$  changes relatively little (Fig. 8), but develops spikes up and down, when  $\rho_0$  approaches  $\rho_0 \approx 0.7$ . The reason is apparent from the variation of  $\epsilon_{xx}^I$  and  $\epsilon_{xx}^{II}$  as function of  $x$ , shown in Figs. 9 and 10. Both  $\epsilon_{xx}^I$  and  $\epsilon_{xx}^{II}$  can become simultaneously

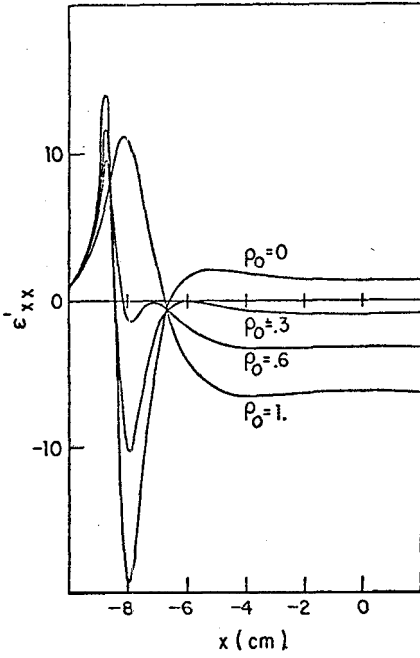


Fig.5 -  $\epsilon'_{xx}$  versus  $x$  for different values of  $\rho_0$ ; distribution function  $f^I$ .

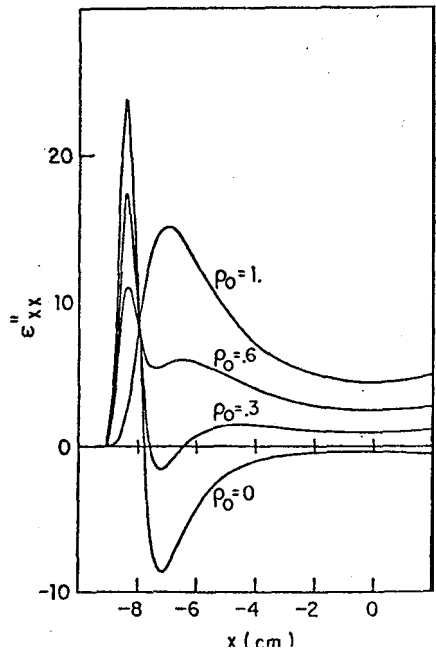


Fig. 6 -  $\epsilon''_{xx}$  versus  $x$  for different values of  $\rho_0$ ; distribution function  $f^I$ .

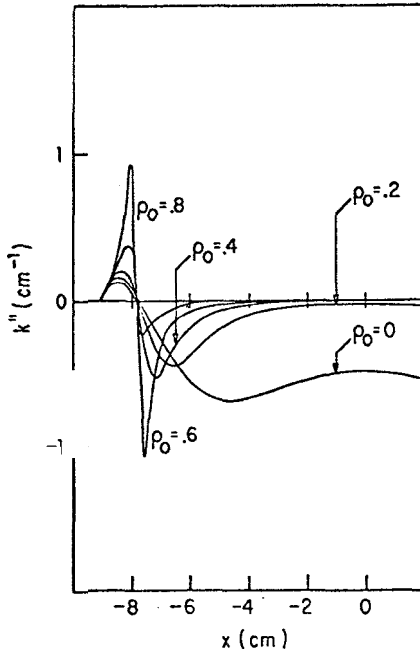


Fig.7 -  $k''$  versus  $x$  for different values of  $\rho_0$ ; distribution function  $f^{II}$ ; for  $\rho_0=1$ , the curve is indistinguishable from the axis.

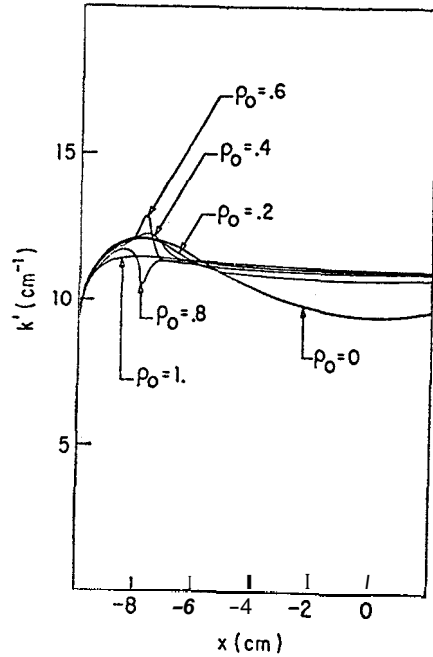


Fig. 8 -  $k'$  versus  $x$  for different values of  $\rho_0$ ; distribution function  $f^{II}$ .

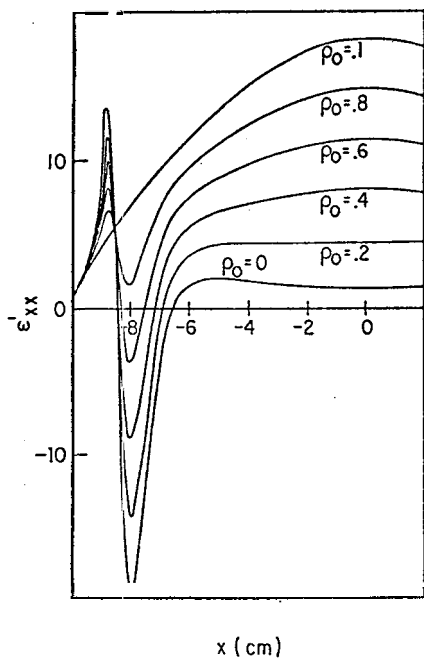


Fig.9 -  $\epsilon'_{xx}$  versus  $x$ , for different values of  $\rho_0$ ; distribution function  $f^{II}$ .

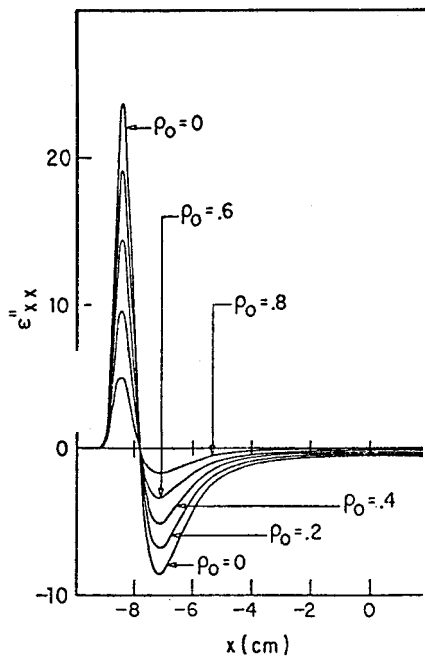


Fig. 10 -  $\epsilon''_{xx}$  versus  $x$  for different values of  $\rho_0$ ; distribution function  $f^{II}$ ; for  $\rho_0 = 1$ , the curve is indistinguishable from the axis.

zero near  $x = -7.8$  cm, when  $\rho_0 \approx 0.7$ , and the argument proceeds as stated previously for  $f^I$ .

Another aspect which should be noted in the behavior of  $k''$  (Fig. 7) is the large reduction of its value over most of the slab, even for small values of  $\rho_0$ . One would expect that a small reduction in the density of loss-cone particles, and their substitution by Maxwellian particles of much lower temperature, should be almost irrelevant. One must realize, however, that for the parameters and profiles chosen for the Maxwellian particles the condition  $X > v_e/c$  is satisfied across the slab, and that dielectric effects are therefore important<sup>4</sup>. These effects are taken into account by multiplying the independent particle expression for  $k''$ <sup>5</sup> by the factor<sup>4</sup>  $\frac{1}{N^T} |(\epsilon_{xx} - i\epsilon_{xy})/\epsilon_{xx}|^2$ . The anti-hermitian part of  $\epsilon_{xx}$ , due to the resonance  $\delta$  function, contains the factor  $\exp\{\mu_{1,\ell}(1-Y^2)/2\}$ , and does not change appreciably with the admixture of the Maxwellian particles, because  $\mu_{1,0} \gg \mu_{1,3}$ ; essentially, it changes in proportion to the density of loss cone-particles (Fig.10). But  $\epsilon'_{xx}$  (Fig.9) and  $\epsilon'_{xy}$ , for which the integration is weighted by the entire distribution function, are much more sensitive to the change of  $\rho_0$  resulting in an impressive effect on  $k''$ .

Some values of the amplification  $A_{\rho_0}$  are shown in Table 2. The reduction in emission is evident also in this case. As  $\rho_0$  approaches 1, the distribution becomes so cold that the emission is negligible at the frequency considered (as was shown in Ref.1, the range of frequencies which are amplified or absorbed moves away from the cyclotron frequency when the temperature increases, and the width of the range of interacting frequencies grows with temperature).

Finally we discuss a feature pertaining to both types of distributions considered, namely the occurrence of marked variations of  $k'$  for certain values of  $\rho_0$  (see Figs. 3 and 8). This contradicts a commonly held belief that  $k'$  is almost insensitive to the shape of the momentum distribution function, and that therefore the cold plasma result is always a good approximation to  $k'$  when frequencies are not too close to the upper hybrid one; our results bear out these features over a large range of values of  $\rho_0$ . But for those values of  $\rho_0$  for which  $\epsilon_{xx}$  approaches zero (i.e., for which both  $\epsilon'_{xx}$  and  $\epsilon''_{xx}$  change sign at nearly the same point in the slab), the value of  $k'$  varies appreciably with  $\rho_0$ , i.e., with the shape of  $f(\vec{p})$  ( $\epsilon_{xx} = 0$  is, by

Table 2 -  $A_{\rho_0}$  for several values of  $\rho_0$  ;  
distribution function  $f^{II}$ .

| $\rho_0$ | $A_{\rho_0}$ |
|----------|--------------|
| 0        | 0.0          |
| 0.1      | -39.5        |
| 0.2      | -49.3        |
| 0.9      | -70.7        |
| 0.95     | -74.5        |
| 0.98     | -78.8        |
| 0.99     | -82.2        |

the way, the perpendicular cold plasma resonance condition for the extraordinary mode). As an illustration the behaviour of  $k^I$  for  $f^I$  in Fig.3 can be followed simply by considering a point where  $\epsilon_{xx}^{II}$  (and therefore: also  $\epsilon_{xy}^{II}$ ) is zero. We then have from Eq. (4),

$$k^I = \frac{\omega}{c} \left| \frac{\epsilon_{xx}^{I2} - |\epsilon_{xy}^I|^2}{\epsilon_{xx}^I} \right|^{1/2}$$

Therefore, if  $\epsilon_{xx}^I$  is negative and tends to zero, with  $|\epsilon_{xx}^I| < |\epsilon_{xy}^I|$ , then  $k^I$  may become large; if  $\epsilon_{xx}^I$  has a positive small value, with  $|\epsilon_{xx}^I| > |\epsilon_{xy}^I|$ , then  $k^I$  may become small. The first case occurs for  $\rho_0 = 0.3$  near  $x = -6.4$  cm, where  $\epsilon_{xx}^I = -0.3$  and  $\epsilon_{xy}^I = 1.2$  i (as can be seen in Figs. 5 and 11); the second occurs for  $\rho_0 = 0.2$  near  $x = -5.4$  cm, where  $\epsilon_{xx}^I = 0.49$  and  $\epsilon_{xy}^I = 0.39$  i.

An analysis of the ordinary mode will not be given here, mainly because it is similar but presents much smaller values of  $k^{II}$  for the parameters chosen, resulting in much smaller magnitude of amplification. We only remark that the behavior of  $k^{II}$  is smooth for the ordinary mode, and the reason is apparent from the expression for  $k^{II}$ , resulting from Eq. (4)

$$N_O^{II} = (1/2N_O^I)(\epsilon_{zzO} \chi_{zz}^{II}) / \left[ (1 - \chi_{zz}^I)^2 + \chi_{zz}^{I2} \right]$$

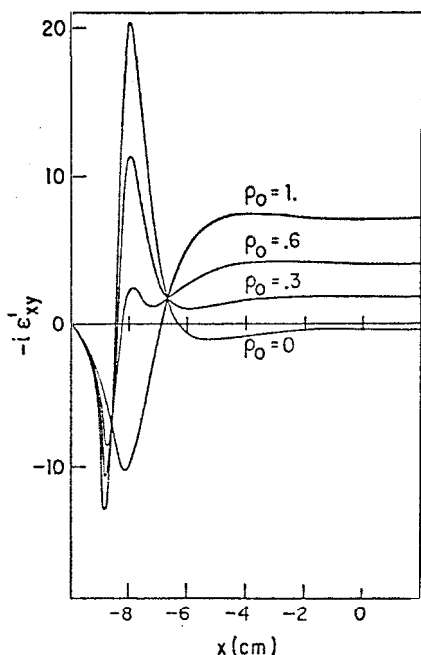


Fig.11 -  $\epsilon'_{xy}$  versus  $x$  for different values of  $\rho_0$ , distribution function  $f^I$ .

The elements  $\chi'_{zz}$  and  $\chi''_{zz}$  have a smooth behavior in  $x$ , and have magnitudes smaller than 1, both for  $f^I$  and  $f^{II}$  distributions. As  $N'_0$  is very close to the value obtained in the cold plasma approximation,  $N'_0$  shows no sharp changes in value.

We sum up the results of the present work in the following conclusions regarding the extraordinary mode. For distributions of type  $f^I$ , even a small degree of filling up of the loss cone can give rise to very effective absorption near the central region, in contrast to the amplification obtained in the pure loss cone case. When the Maxwellian situation is approached, the amplification disappears and absorption occurs over almost the entire slab. For distributions of type  $f^{II}$ , the presence of the very cold Maxwellian component reduces the amplification while producing no appreciable absorption at the frequency considered, so that the emission becomes negligible when the cold component is completely dominant. For both types of distributions the transition to a purely Maxwellian one can be accompanied by large localized variation in the imaginary and real parts of the propagation vector, which may invalidate the use of the geometrical optics approximation, pointing to the need of some care in assuming



that, if one is away from the upper hybrid frequency, the index of refraction for the extraordinary mode is independent of the momentum distribution. This result is not restricted to the particular examples treated, or to the particular form of the distribution function used; it is connected to the fact that  $\epsilon'_{xx}$  can become very small or even change sign inside the plasma and to the existence of a population inversion in the distribution function. Therefore, it may be of significance in the study of non-equilibrium thermonuclear plasmas.

This work was supported by grants from Conselho Nacional de Desenvolvimento Científico e Tecnológico and Financiadora de Estudos e Projetos, Brasil. Useful comments by C.S.Wu and I.Fidone are gladly acknowledged.

#### REFERENCES

1. L.F.Ziebell and D.Dillenburg, Phys. Fluids, 26, 80 (1983).
2. M.A.Lieberman, A.J.Lichtenberg and T.Takeshita, Plasma Phys. 13,141 (1971).
3. H.Kubo, S.Nakamura, T.Yuyama, M.Hosokawa, S.Aihara and H.Ikegami, J.Phys.Soc.Jap. 45, 1372 (1978).
4. I.Fidone, G.Granata, R.L.Meyer, E.H.Jornada, R.S.Schneider and L.F.Ziebell, Phys. Fluids 23, 1336 (1980).
5. G.Bekefi, *Radiation Processes in Plasma* (Wiley, New York, 1966).
6. V.D.Shafranov, in *Review of Plasma Physics*, edited by M.A.Leontovitch (Consultants Bureau, New York, 1967), Vol.3, p.75.
7. K.R.Chu and B.Hui, Phys. Fluids, 26, 69 (1983).

#### Resumo

Investigamos a amplificação de ondas de cíclotron eletrônicas em uma lâmina inhomogênea de plasma, como função da distribuição de momentum dos elétrons. Consideramos dois tipos de distribuições, ambas apresentando uma componente tipo cone de perda e uma componente Maxwelliana. Mostramos que a emissão perpendicular na frequência fundamental é em geral grandemente reduzida pela presença de uma componente Maxwelliana e que ocorrem situações em que uma camada da lâmina absorve muito eficazmente toda a radiação já amplificada no restante do plasma. A transição do caso cone de perda puro para o caso Maxwelliano puro é acompanhada por um comportamento peculiar das compo-

nentes do tensor dielétrico, comportamento esse que pode invalidar a aproximação da ótica geométrica no cálculo da emissão e também a crença comum de que a parte real do índice de refração é insensível à forma da função distribuição.